



HAL
open science

In Operando Spectroscopic Ellipsometry Investigation of MOF Thin Films for the Selective Capture of Acetic Acid

Sanchari Dasgupta, Subharanjan Biswas, Kevin Dedecker, Eddy Dumas, Nicolas Menguy, Bruno Berini, Bertrand Lavedrine, Christian Serre, Cédric Boissière, Nathalie Steunou

► **To cite this version:**

Sanchari Dasgupta, Subharanjan Biswas, Kevin Dedecker, Eddy Dumas, Nicolas Menguy, et al.. In Operando Spectroscopic Ellipsometry Investigation of MOF Thin Films for the Selective Capture of Acetic Acid. ACS Applied Materials & Interfaces, 2023, 10.1021/acsami.2c17682 . hal-03954450

HAL Id: hal-03954450

<https://hal.sorbonne-universite.fr/hal-03954450v1>

Submitted on 24 Jan 2023

HAL is a multi-disciplinary open access archive for the deposit and dissemination of scientific research documents, whether they are published or not. The documents may come from teaching and research institutions in France or abroad, or from public or private research centers.

L'archive ouverte pluridisciplinaire **HAL**, est destinée au dépôt et à la diffusion de documents scientifiques de niveau recherche, publiés ou non, émanant des établissements d'enseignement et de recherche français ou étrangers, des laboratoires publics ou privés.

In Operando Spectroscopic Ellipsometry Investigation of MOF Thin Films for the Selective Capture of Acetic Acid.

Sanchari Dasgupta,^{†,||} Subharanjan Biswas,^{†,||} Kevin Dedecker,[†] Eddy Dumas,[†] Nicolas Menguy,[‡] Bruno Berini,[‡] Bertrand Lavedrine,[‡] Christian Serre,^{*,‡,§} Cédric Boissière^{*,§} and Nathalie Steunou.^{*,†}

[†] Institut Lavoisier de Versailles, UMR CNRS 8180, Université de Versailles St Quentin en Yvelines, Université Paris Saclay, 78035 Versailles, France.

[‡] Sorbonne Université, UMR CNRS 7590, MNHN, IRD, Institut de Minéralogie, de Physique des Matériaux et de Cosmochimie, IMPMC, 75005 Paris, France

[‡] Groupe d'Etudes de la Matière Condensée, UMR CNRS 8635, Université de Versailles St Quentin en Yvelines, Université Paris Saclay 78035 Versailles, France.

[‡] Centre de Recherche sur la Conservation, UAR CNRS 3224, Muséum National d'Histoire Naturelle, 75005 Paris, France.

[‡] Institut des Matériaux Poreux de Paris (IMAP), Ecole Normale Supérieure de Paris, ESPCI Paris, CNRS, PSL University, 75005 Paris, France

[§] Sorbonne Université, CNRS, Collège de France, UMR Chimie de la Matière Condensée de Paris, 75005 Paris, France.

ABSTRACT: The emission of polar volatile organic compounds (VOCs) is a major worldwide concern of air quality and equally impacts the preservation of cultural heritage (CH). The challenge is to design highly efficient adsorbents able to selectively capture traces of VOCs such as acetic acid (AA) in the presence of relative humidity (RH) normally found at storage in museums (40-80%). Although the selective capture of VOCs over water is still challenging, Metal-Organic Frameworks (MOFs) possess highly tunable features (Lewis, Bronsted or redox metal sites, functional groups, hydrophobicity...) suitable to selectively capture a large variety of VOCs. In this context, we have explored the adsorption efficiency of a series of MOFs thin films (ZIF-8(Zn), MIL-101(Cr) and UiO-66(Zr)-2CF₃) for the selective capture of AA based on a UV/Vis and FT-IR spectroscopic ellipsometry in operando study (2-6% of relative pressure of AA under 40% of RH), namely conditions close to the realistic environmental storage conditions of cultural artefacts. For that purpose, optical quality thin films of MOFs were prepared by dip-coating and their AA adsorption capacity and selectivity were evaluated under humid conditions by measuring the variation of the refractive index as a function of the vapor pressures while the chemical nature of the co-adsorbed analytes (water and AA) was identified by FT-IR ellipsometry. While thin films of ZIF-8(Zn) strongly degraded when exposed to AA/water vapors, films of MIL-101(Cr) and UiO-66(Zr)-2CF₃ present a high chemical stability under those conditions. It was shown that MIL-101(Cr) presents a high AA adsorption capacity due to its high pore volume, but exhibits a poor AA adsorption selectivity under humid conditions. In contrast, UiO-66(Zr)-2CF₃ was shown to overpass MIL-101(Cr) in terms of AA/ H₂O adsorption selectivity and AA adsorption/desorption cycling stability thanks to its high hydrophobic character, suitable pore size for adequate confinement and specific interactions.

KEYWORDS: MOFs, volatile organic compounds, adsorption, thin films, ellipsometry

1. INTRODUCTION.

Nowadays, air pollution is a major worldwide concern and a low air quality is often attributed to volatile organic compounds (VOCs) emissions which cause adverse health effects. Cultural heritage (CH) artefacts in museums, archives, libraries and artworks in private collection as well - are threatened and can be severely deteriorated by air pollutants.¹⁻² This issue has attracted the attention of a growing number of conservators and scientists to find new ways for evaluating the risks related to pollutants, the dose-damage relationship and the development of new monitoring techniques.³⁻⁵ Indoor air measurements in CH institutions clearly indicate rather low levels of infiltrated outdoor pollutants but a high quantity of VOCs is emitted by wood, paints, resins, plastic foams, insulating materials, wall and floor coverings, as well as furnishings

often used in museum rooms, storage areas, and showcases.¹⁻² The VOCs are also generated during the degradation of museum artefacts. Analyses performed by the Getty Conservation Institute inside seventeen museums and institutions have shown that acetaldehyde, acetic acid (AA), formaldehyde, and formic acid are the most common carbonyl compounds (CCs) encountered in museums.⁶ Their amount of up to a few 100 ppb strongly depends on the storage materials or the historical objects.⁷⁻⁸ More than 75 years of visual and audio memories made with cellulose derivatives are actually in serious danger due to the hydrolysis and oxidation of cellulose acetate into AA.¹⁻² The mitigation strategies mostly rely on improving the chemical filtration in the air conditioning unit or storing the cultural artefacts in a showcase at low temperature and low RH.^{1-2, 8} However these technologies and protocols are quite expensive, energy-consuming and not effective enough to prevent the irretrievable damage of historical objects with time since they do not allow to maintain a very low tolerated concentration of CCs (typically 400-40 ppb of AA for a 1-100-year preservation target) which is required for museum, gallery, library, and archival collections.¹⁻² A viable solution to protect CH artefacts consists of using adsorbents to efficiently capture CCs. Different adsorbents such as activated carbons, zeolites, silica and pillared clays are currently employed in the context of CH.⁹⁻¹⁰ These commercially available shaped sorbents present the advantage to be easily introduced at the vicinity of an artefact such as in showcases, storage boxes or cabinets and have been to date intensively considered for the capture of many CCs.⁹⁻¹² However, AA is a highly acidic and hydrophilic molecule which raises additional challenges compared to other more hydrophobic CCs, due to its strong competitive adsorption with water under RH above 30%. As a consequence, zeolites and activated carbons suffer from limited AA capture performances since these porous materials are either poorly selective in the presence of humidity (zeolites) and/or show low AA affinity (carbons). This leads on both cases to poor capture performances when traces of AA are present.⁹⁻¹² Therefore, the design of alternative adsorbents highly efficient to selectively adsorb traces of AA in the presence of humidity, i.e. with RH classically ranging in museums from 30 to 60% is still a great challenge for the CH preservation. Note that the development of efficient CCs adsorbents that are used in other indoor environments is also a major public health concern for the air quality.

In the continuous quest of valuable solutions for air quality, Metal-Organic Frameworks (MOFs) are recognized as an emerging class of adsorbents toward the abatement of VOCs including CCs owing to their large surface area and chemical functionality.¹³⁻¹⁶ Specific adsorption sites can be introduced in the MOF backbone either on their inorganic nodes (Lewis acid groups) or through the introduction of functional groups ($-\text{CF}_3$, -alkyl chain or $-\text{NH}_2$) on the organic linker. Their chemical diversity, tuneable hydrophobicity/hydrophilicity balance and selective sorption properties are thus exploited to optimize the host/guest interactions involved in numerous applications including gas storage, gas/liquid separation, sensing, energy conversion/storage, catalysis.^{13, 17-18} MOFs have also been considered for the capture and catalytic degradation of toxic industrial chemicals, chemical warfare agents and also environmental VOCs, even at trace levels in ambient condi-

tions.¹⁹⁻²² However, until now, only a few studies have been reported on MOFs for CCs capture under humid conditions.²³⁻²⁶ Notably, most of the previously reported works have studied the efficiency of MOFs for the removal of only a single CC (most prominently formaldehyde)²⁴ while CCs are present in the indoor environment as a gaseous mixture in which water is the most abundant interfering species. As a consequence, it is noteworthy that only MOFs with a high chemical and water stability should be considered for the selective capture of VOCs under humid ambient conditions. However, in the past few years, different strategies have been reported to design chemically stable MOFs such as porous polycarboxylates based on high valent cations (Zr^{4+} , Ti^{4+}).²⁷⁻²⁸ Recently, some of us have investigated the use of MOFs for the capture of AA in the presence of water (40% RH), considering an environmental chamber.¹⁹ This previous work has led to the identification of several MOFs such as ZIF-8(Zn), MIL-140B(Zr), MIL-101(Cr) and UiO-66(Zr)-2CF₃ that were shown to capture traces of AA in the presence of humidity, thereby overpassing the benchmark RB4 activated carbon for this application.¹⁹ The performance of such adsorbents was mainly evaluated by the measurement of the residual amount of AA in the environmental chamber after 2 hours of exposure and thus from their capacity to remove AA. However, the characterization of their AA/water co-adsorption properties under the real conditions of the application (nature of the adsorbed species) as well as the evaluation of their adsorption/desorption cyclability and thus their long-term reusability were not investigated. Note that AA sorption isotherms as single component of MOFs cannot evaluate the efficiency of MOFs for the selective capture AA under humid conditions since the competitive adsorption of water not only decreases their AA adsorption capacity but may also impact the hydrophilic-hydrophobic balance of the materials and thus their AA affinity. The potential of these MOFs as AA sensors was also not explored.

In this paper, we explored the competitive sorption behavior of a few of these MOFs, as thin films, exposed to AA/water vapor through environmental ellipsometric porosimetry. This technique is a very powerful characterization method for nanoporous optical films.²⁹ As previously reported, UV-visible spectroscopic ellipsometry (UVSE) was capable to fully characterize the porosity, the mechanical properties and the –sorption properties of micro- and mesoporous films (oxides and MOFs) under a controlled atmosphere and at various temperatures.³⁰⁻³¹ The processing of MOF thin films has been reported by numerous strategies including layer-by-layer approach, vapor phase conversion of oxide, electrochemistry and so on.^{13, 17, 32} UVSE requires the processing of thin films of high optical quality that are typically obtained through the deposition of stable colloidal suspension of nanoparticles (NPs) with particle size lower than 100 nm. The adsorption properties of a few MOFs (i. e. MIL-101(Cr), ZIF-8(Zn), MIL-89(Fe)) for different vapors (i.e. isopropanol, THF, n-heptane, iso-octane, cyclohexane and water) were previously studied by some of us with the use of UVSE.³⁰⁻³¹ This experiment involves the *in situ* monitoring of the refractive index in UV-Vis spectral range and the thickness of the film upon variation of the relative vapor pressure between 0 % and 100 % inside the analysis chamber. Note that UVSE experiments can be performed at RT and does

not require any activation of the material in comparison to standard sorption experiments. It is thus a valuable tool to characterize the co-adsorption properties of MOFs using *in operando* conditions, namely conditions close to the realistic environmental storage conditions of cultural artefacts. This technique may thus provide valuable information on the affinity of a sorbent towards a mixture of vapors which is much more complex to extract from standard sorption experiments. In the present case, we have performed these experiments on MOF thin films of high optical quality. The selected MOFs (i. e. ZIF-8(Zn), MIL-101(Cr) and UiO-66(Zr)-2CF₃) can be synthesized as monodisperse nanoparticles. They present a good chemical stability and high hydrophobic character that may limit the co-adsorption of water. UVSE experiments have allowed us to fully describe the AA/H₂O co-adsorption and adsorption/desorption cycling properties of these MOF thin films. In addition, the composition of the co-adsorbed species (vibrational signature in IR range) in the MOFs pores was monitored as a function of the vapor pressures and time by *in situ* IR spectroscopic ellipsometry (IRVASE).³³ In light of the results obtained from this synergistic combination of UV-Vis and FT-IR spectroscopic ellipsometry platform, it was possible to elucidate the interactions between MOFs and adsorbed species (AA and water) and thus a fundamental understanding of the water/AA co-adsorption processes of these MOFs was achieved. While a competitive AA/H₂O co-adsorption process was evidenced for MIL-101(Cr), UiO-66(Zr)-2CF₃ was shown to selectively adsorb AA under humid ambient conditions and could thus be used as a highly performing CH adsorbent. To the best of our knowledge, this work provides the first detailed evaluation of the adsorption and detection performance of MOFs towards AA under competing humidity conditions and these findings will be helpful for the future development of highly performing VOCs adsorbents.

2. EXPERIMENTAL SECTION.

2.1. Processing of MOF thin films. The preparation of MOF thin films was carried out by dip-coating process. For each MOF, a colloidal solution of MOF nanoparticles (NPs), denoted nanoMOF, was prepared at 0.01 mol.L⁻¹ in ethanol. Thin films of nanoMOFs were prepared by dip-coating these colloidal solutions under ambient conditions (room temperature (RT), atmospheric pressure) by using a silicon wafer previously washed with ethanol. The withdrawal speed was set at 0.05 or 15 mm s⁻¹. At the end of the nanoMOF deposition, the silicon plate is left for 1 min at RT for the evaporation of the remaining solvent. To stabilize the freshly deposited coating, the films were then heated at 120°C for 2 min with a heating ramp of 18 °C.min⁻¹ and then cooled down before the adsorption experiment.

2.2. Characterization. X-ray powder diffraction patterns of nanoMOF and films were acquired with a D5000 Siemens X'Pert MDP diffractometer for a range of 2θ from 5 to 30°. The porosity of nanoMOFs was characterized by nitrogen porosimetry at 77 K by using a BELSORP-Mini porosimeter. A Perkins Elmer SDA 6000 apparatus was used for the thermogravimetric analysis. The samples were heated up to 600°C with a temperature ramp of 5°C.min⁻¹ under a flow of air.

Colloidal solutions of MOFs were characterized by dynamic light scattering (DLS) experiments with a Malvern nanosizer (Nano ZS). For TEM characterization, samples were prepared by depositing one droplet of the colloidal suspension onto a carbon-coated copper grid and left to dry in air. TEM observations were performed using a JEOL 2010 Transmission Electron Microscope operating at 200 kV. High-angle annular dark field imaging in scanning transmission electron microscope mode (STEM-HAADF) was performed on a JEOL JEM 2100F microscope installed at IMPMC (Paris, France), operating at 200 kV, equipped with a field emission gun, a JEOL detector with an ultrathin window allowing detection of light elements and a scanning TEM (STEM) device, which allows Z-contrast imaging in HAADF mode. SEM images have been recorded on a JEOL JSM-7001F microscope using gold-coated samples equipped with an X-ray energy-dispersive spectrometry (XEDS) detector with a X-Max SDD (silicon drift detector) by Oxford. Atomic Force Microscopy (AFM) was carried out in air with a Dimension ICON (Bruker) microscope, more precisely with the Peak Force tapping mode. For this purpose, a silicon tip on nitride lever (ScanAsyst Air model, Bruker) with a 0.4 N/m spring constant and a nominal tip radius of 2 nm was used with a resolution of 512 pixels x 512 pixels.

2.3. Characterization of the sorption properties of MOF films by UV-visible (UVSE) and IR spectroscopic ellipsometry (IRVASE). The UVSE experiments were performed with a UV-Vis (from 245 to 1000 nm) variable angle ellipsometer (Woollam M-2000U) and the Complete EASE software using Cauchy models. The IRVASE experiments were conducted with A MARK-II IRVASE from Woolam Company. FTIR extraction was performed by using a “wavelength by wavelength” model inversion after having fixed thin film thickness (obtained from UVSE analysis). These experiments required a chamber containing the nanoMOF film equipped with a THMSEL600 heat cell (from Linkam company) for the in-situ monitoring of film refractive index in the presence of AA/water vapor mixtures (Figures S22 and S23). After moderate heating (120°C for 10 minutes) and cooling in dry air, the AA and water vapor mixed atmosphere was injected into the analysis chamber for adsorption experiments (air/water/AA proportions were controlled with two pairs of mass flow controller from Sol-Gel Ways Company (Figure S22)).

3. RESULTS AND DISCUSSION.

3.1. Synthesis of nanoMOFs and processing of thin films. In this article, we have considered first the slightly hydrophobic mesoporous chromium terephthalate, MIL-101(Cr) (cage dimensions of 2.9 and 3.4 nm), owing to the presence of coordinatively unsaturated metal sites (Lewis acid sites) that can potentially act as strong AA adsorption sites and to its very large pore volume allowing high and fast AA uptake.³⁴ We have also selected the microporous hydrophobic Zn

imidazolate (cavities of 11.6 Å).³⁵ Finally, the microporous three-dimensional Zr dicarboxylate, UiO-66(Zr)-2CF₃ (tetrahedral and octahedral cage dimensions of 0.8 and 1.0 nm, respectively) bearing pending -CF₃ groups substituted in the terephthalate linker was also considered.¹⁹

For the analysis of films by ellipsometry, the film rugosity must indeed be as low as possible which implies the processing of MOF films with nanoMOF particle size diameter usually below 100 nm. ZIF-8(Zn) and MIL-101(Cr) nanoparticles (NPs) were synthesized following synthesis protocols already available in literature (see supporting information (SI)).³⁰⁻³¹ In this work, the synthesis of UiO-66(Zr)-2CF₃ NPs was slightly adapted from a previously solvothermal protocol,³⁶ relying here on ambient pressure round-bottom flask protocol suitable for a larger scale production. To obtain stable UiO-66(Zr)-2CF₃ colloidal solutions, a monodentate modulator, i.e. benzoic acid and moderate temperature synthesis (60°C), were considered. As previously shown, these molecules compete with the organic linker for coordination with the metal cation which strongly affects the nucleation kinetics of the MOF and thus enable to tune the particle diameter of the MOF.³⁷⁻³⁹ Moreover, the introduction of a benzoic acid in the reaction medium can also induce the presence of missing linker defects.^{37, 40} Thus, UiO-66(Zr)-2CF₃ NPs were synthesized by heating at 60°C the precursors (ZrOCl₂.8H₂O and 2,5-bis(trifluoromethyl)terephthalic acid) with an excess of acids (benzoic acid and HCl) in DMF (see SI for more details). All nanoMOFs were then characterized by combining powder X-ray diffraction (PXRD) (Figures S1, S2 & S3), N₂ porosimetry (Figures S4, S5 & S6), thermogravimetric analysis (TGA) (Figures S7, S8 & S9) and FTIR spectroscopy (Figures S10, S11 & S12). PXRD showed the characteristic Bragg peaks of MOF with a substantial broadening, in agreement with the presence of NPs. FT-IR and TGA did not evidence the presence of any impurity such as unreacted organic linker or metal oxides. According to TEM and HAADF-STEM experiments (Figure S13) ZIF-8(Zn) nanocrystals with a diameter of 40±10 nm were synthesized with a characteristic rhombic dodecahedral shape as previously reported.⁴¹ Spheroidal small nanocrystals were obtained for MIL-101(Cr) and UiO-66(Zr)-2CF₃ with a diameter of 30 ± 15 nm and 20 ± 15 nm respectively (Figures S13 and S14). SEM-XEDS mapping experiments (Figures S15 and S16) show the homogeneous chemical composition of the MOF samples.

Stable colloidal solutions of these nanoMOFs could then be prepared through the dispersion of NPs in ethanol at a concentration of 0.01 mol. L⁻¹ as shown by dynamic light scattering (Figures S17, S18 & S19). The elaboration of thin film of optical quality is required for their characterization by UV-vis ellipsometry. As previously demonstrated, the thickness and microstructure of MOF films strongly depend on the concentration of MOF colloidal solution, temperature and withdrawal speed.³⁰⁻³¹ This latter leads to two different mechanisms of deposition called draining (> 1 mm s⁻¹) and capillary regimes (< 0.1 mm s⁻¹) including an intermediate regime (0.1-1 mm s⁻¹). As previously shown on ZIF-8(Zn) and MIL-101(Cr) films,³⁰⁻³¹ the deposition of MOFs solutions in the capillary regime can lead to thin films of high optical quality with a limited rough-

ness due to the homogeneous distribution of densely packed MOF NPs on the glass substrate. Thin films of the nanoMOFs were thus prepared following a single deposition process of a 0.01 mol.L^{-1} colloidal solution of nanoMOF at a withdrawal speed of 0.05 mm.s^{-1} . As measured by UVSE, the film thickness of MIL-101(Cr), ZIF-8(Zn), and UiO-66(Zr)-2CF₃ were respectively equal to 289, 312 and 146 nm. AFM experiments were performed to characterize the morphology of the thin films (see Figure 1). These films are covered by a uniform and homogeneous distribution of densely packed MOF nanocrystals. The root-mean-square roughness was estimated to be close to 18 nm, 15 nm and 10 nm for thin films of MIL-101(Cr), ZIF-8(Zn), and UiO-66(Zr)-2CF₃ respectively.

3.2. Adsorption of acetic acid by ZIF-8(Zn) thin films. The AA adsorption properties of thin films of nanoMOFs in the presence of humidity were first investigated by in situ UVSE under ambient conditions (RT, 1 bar) close to the real museum environment. First, the co-adsorption properties of ZIF-8(Zn) towards AA/water mixtures was evaluated. The experiment was conducted at RT into three steps. First, a water vapor flow was injected into a chamber containing the film to reach 40% RH. Then, an air flow containing 2% relative pressure (P/P_{vapsat}) of AA (296 ppm) was injected leading to a chamber with 40% RH and 2% P/P_{vapsat} of AA. Finally, the desorption occurred by dry air flushing. Due to the high hydrophobicity of ZIF-8(Zn), the change of refractive index (RI) was low ($\Delta\text{RI} = 0.02$) under water vapor (Figure 2(A)). In the presence of AA vapor, a very fast increase of RI up to $n(700 \text{ nm}) = 1.55$ ($\Delta\text{RI} = 0.40$) was observed. However, after desorption, the RI decreased slightly but did not reach its initial value. Therefore, an irreversible phenomenon occurred during the adsorption experiment. The initial ZIF-8(Zn) film was iridescent before the experiment, due to interferences between the MOF film and the substrate. After exposure to water/AA vapors, it became strongly tarnished. The comparison of the PXRD pattern before and after the exposure to the mixture of water/AA showed that the ZIF-8(Zn) crystalline structure was totally degraded upon the exposure to AA/water vapor mixtures (Figure 2(B)). As previously reported, ZIF-8(Zn) NPs, films and membranes can degrade under humid conditions, as a result of the hydrolysis of Zn-N bonds.⁴¹⁻⁴³ These results show that a mixture of water/AA vapor affects dramatically the crystalline structure of ZIF-8(Zn). This is tentatively associated with a decrease of the internal hydrophobicity of this MOF as a result of attractive interactions (H-bonds and Van der Waals) between -COOH groups from AA adsorbed within the structure and water molecules. This cooperative AA/water co-adsorption changes drastically the hydrophobic-hydrophilic balance of the MOF, thus its reactivity towards water hydrolysis. Although this falls out of the scope of this study, this quick and massive increase of RI upon AA exposure makes the nano-ZIF-8(Zn) films interesting candidates for the design of highly sensitive single-use AA sensor in presence of humidity.

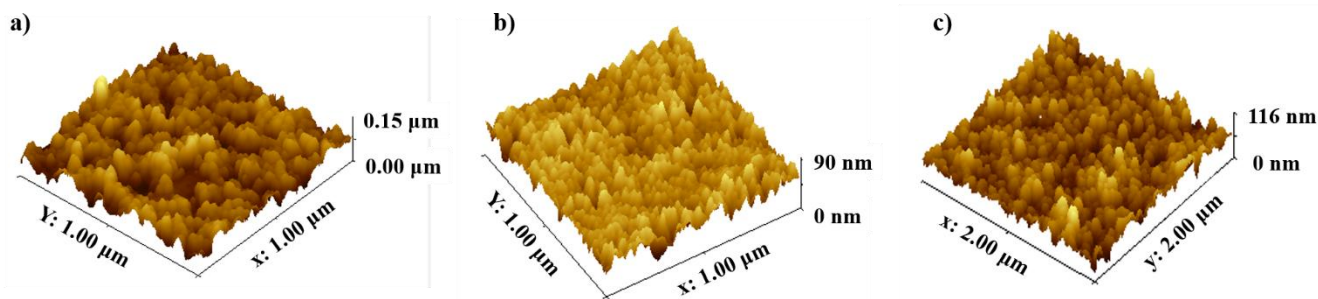


Figure 1. AFM images of a) MIL-101(Cr), b) UiO-66(Zr)-2CF₃, c) ZIF-8(Zn) thin films

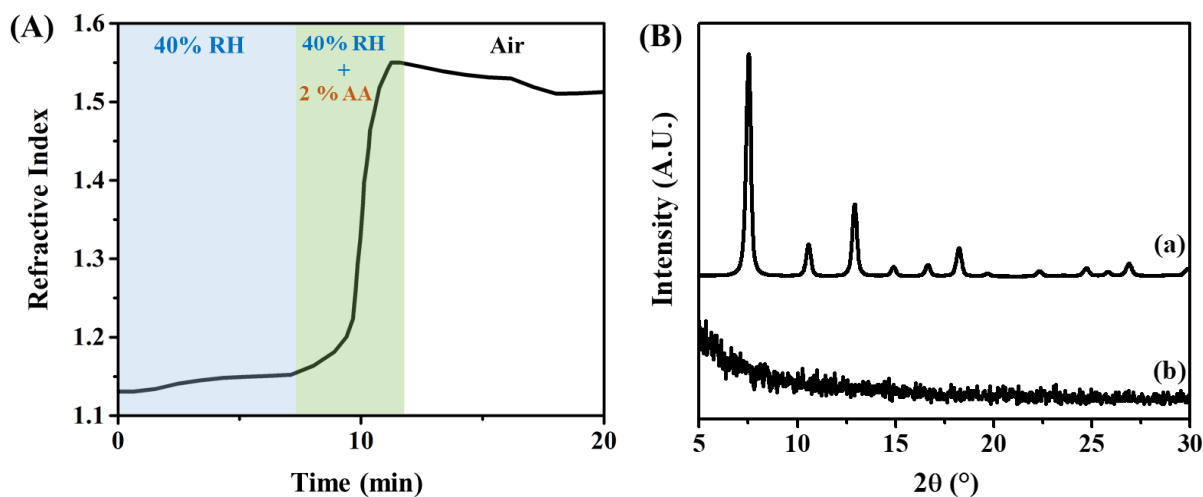


Figure 2. (A) RI evolution of ZIF-8(Zn) thin films exposed to sequential different environments namely 40% RH, 2% of AA and 40% RH and dry air. (B) PXRD pattern of ZIF-8(Zn) films (a) before and (b) after exposure to AA/water vapors.

3.3. Characterization of the water/AA co-adsorption properties of MIL-101(Cr) and UiO-66(Zr)-2CF₃ films by UV-vis and infrared spectroscopic ellipsometry. The chemical stability of both MOFs in the presence of AA/water mixture was first evaluated by PXRD. Both powdered MOF samples were thus exposed in an environmental chamber with 40% relative humidity and 2% relative pressure (P/P_{vapsat}) of AA (296 ppm). The PXRD patterns of both MIL-101(Cr) and UiO-66(Zr)-2CF₃ exposed to AA/water mixture for about 2h are identical to that of MOFs initially synthesized (see Figures S20 and S21 of the SI). The crystallinity of these MOFs is not affected after exposure to AA/water mixture. These experiments confirm that both MIL-101(Cr) and UiO-66(Zr)-2CF₃ are chemically stable upon AA adsorption in the presence of humidity. The AA adsorption properties of thin films of MIL-101(Cr) and UiO-66(Zr)-2CF₃ in the presence of humidity were evaluated by UVSE under ambient conditions (RT, 1 bar). First, water adsorption isotherm of MIL-101(Cr) (Figure 3) was measured showing a progressive increase of the refractive index of the MOF film as a result of the adsorption of water molecules in the mesoporous cages (diameter of 29 and 34 Å) of the MOF (at RH = 40%) and in the interparticle mesoporosity (RH > 80%).

This water adsorption isotherm of MIL-101(Cr) thin film is fully consistent with that of water isotherm volumetrically measured on powdered MIL-101(Cr) sample as previously reported.⁴⁴ The water isotherm of UiO-66(Zr)-2CF₃ is characterized by a small increase of RI between 40 and 60% RH ($\Delta RI=0.05$). It is fully consistent with that of water isotherm volumetrically measured on powdered UiO-66(Zr)-2CF₃ as previously reported.¹⁹ Interestingly, it confirmed that the water uptake of UiO-66(Zr)-2CF₃ in conditions of relative humidity found in museum is limited, as previously shown,¹⁹ in agreement with its hydrophobic character. Water adsorption isotherm were then measured by UVSE while maintaining a constant P/P_{vapsat} of AA of 2%. In those conditions, the water adsorption isotherms of both MIL-101(Cr) and UiO-66(Zr)-2CF₃ are however strikingly different. When exposed to the AA/water mixture, MIL-101(Cr) exhibited a higher adsorption below 40% RH than in the absence of AA (Figure 3). Hence, the hydrophilic character of this MOF increased in contact with AA vapor which is likely due to favorable interactions between AA and water as result of a cooperative adsorption process. This is consistent with previous results observed for hydrophobic mesoporous silica exposed to ethanol/water mixtures.⁴⁵ In contrast, at high relative humidity, a lower amount of water was adsorbed into MIL-101(Cr) film in presence of AA, which might be due to an increase of the hydrophobic character of the external surface of NPs. This can be explained with a possible substitution of water molecules coordinated to surface Cr sites of MIL-101(Cr) by AA molecules. Indeed, CCs such as ketones are prone to interact with coordinatively unsaturated sites (CUS) of MOFs such as the mesoporous MIL-100(Fe).⁴⁶ This was also shown here by Infrared spectroscopic ellipsometry (IRVASE). Indeed, IRVASE was used to provide a chemical characterization of the MIL-101(Cr) film upon co-adsorption. Figure 4 displays FT-IR spectra in the 1000-1800 cm⁻¹ region of MIL-101(Cr) films exposed to water/AA vapors of different composition. Under low humidity conditions (RH 5%), the FT-IR spectrum displays the characteristic stretching vibrations of the coordinating carboxylate groups of the terephthalate linker (i. e. $\nu_s(\text{C=O})=1400 \text{ cm}^{-1}$ and $\nu_{\text{as}}(\text{C=O})=1623 \text{ cm}^{-1}$) as also shown in the FT-IR spectrum of the pure MIL-101(Cr) NPs (see Figure S11).⁴⁷ Increasing the RH to 40% leads to the shift of the maximum of this peak to 1631 cm⁻¹ that can be due to the presence of H-O-H bending mode of free water molecules.

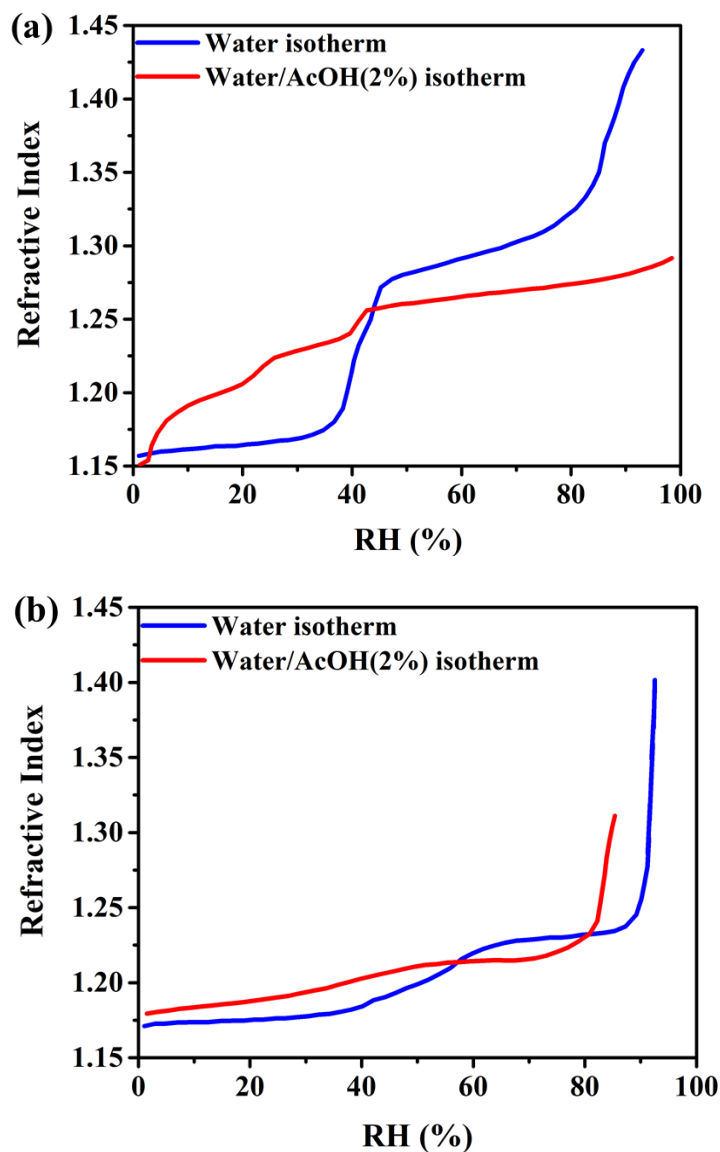


Figure 3. Water adsorption isotherm of (a) MIL-101(Cr) film and (b) UiO-66(Zr)-2CF₃ films exposed to water vapors (RH 40%) and a mixture of water vapors at 40% RH and AA vapors at 2% P/P_{vapsat}. Refractive index is given at 700 nm wavelength.

By deconvoluting these FT-IR spectra, one could detail the impact of AA vapor onto water adsorption. In particular, the 1580-1680 cm⁻¹ region was deconvoluted with the two contributions centered at 1623 and 1640 cm⁻¹ corresponding respectively to the coordinating carboxylate groups and water molecules. This analysis was completed with the analysis of the surface area absorption band of OH stretching groups (from 3000 to 3600 cm⁻¹) (Figure 4c and Figure S24). In the absence of AA, a very little amount of free water was adsorbed into MIL-101(Cr) for RH < 40%. Once MIL-101(Cr) films were exposed to an increasing amount of AA at 40% RH, strong modifications of the FT-IR spectra were observed. The vibration band at 1400 cm⁻¹ became more intense but its analysis is quite complex due to the simultaneous presence of strong vibration

modes associated to the OH and C=O groups of free AA. Vibration bands at 1259 and 1715 cm^{-1} appeared at AA concentrations as low as 1% and their surface area increases with the AA concentration. These bands could be respectively assigned to the $\nu(\text{C-O})$ and $\nu(\text{C=O})$ modes of free AA. This observation is in agreement with the increase of the surface area of the broad vibration band $\nu(\text{O-H})$ in the 3000-3500 range (Figure S24). Remarkably, both the surface area of 1640 and 1623 cm^{-1} bands assigned to free water and coordinated carboxylate groups increased with AA content up to 2% and 6% of AA respectively. This is consistent with (i) an important co-adsorption of water driven by the presence of AA and with (ii) the increasing amount of acetate groups coordinated on the metal sites since the vibration modes of coordinating carboxylate groups of the terephthalate linker overlap with those of complexed acetate groups (i.e. $\nu_s(\text{C=O})$ and $\nu_s(\text{C=O})$). Overall, these results show that a significant amount of AA molecules interact with the coordinatively unsaturated Cr sites (CUS) of MIL-101(Cr) while the majority of AA molecules is also adsorbed in the MOF matrix through weak Van der Waals and hydrogen bond interactions. A similar interaction between the carbonyl function of CCs with open metal sites of MOFs was previously reported.^{25, 46}

UVSE experiments were also performed with the UiO-66(Zr)-2CF₃ thin film. Figure 3(b) shows the water/AA adsorption isotherm of UiO-66(Zr)-2CF₃. Similarly, to MIL-101(Cr), an increase of RI at RH lower than 40% was observed in the presence of AA but to a much lesser extent in comparison to MIL-101(Cr). The low water uptake of UiO-66(Zr)-2CF₃ is fully consistent with its hydrophobic character that prevents water molecules from fully entering the porosity even in the presence of AA. These films were also characterized by IRVASE experiments. As shown in Figure S25, FT-IR spectra of UiO-66(Zr)-2CF₃ films exposed to water vapor of increasing RH were almost identical, in full agreement with the lower affinity of this MOF toward water. Similar FT-IR spectra were also recorded after adsorption/desorption cycles, thereby showing the excellent stability of this MOF under humidity as previously reported.^{19, 48} Figure 4(b) displays FT-IR spectra of UiO-66(Zr)-2CF₃ films exposed to a variable amount of AA at 40% RH. Similarly, to MIL-101(Cr), the presence of free AA is clearly identified by the appearance of strong vibration bands at 1708, 1270 and 1305 cm^{-1} , their intensity increasing with the AA amount. The intensity of the vibration bands of the coordinated terephthalate ($\nu_s(\text{C=O})=1388 \text{ cm}^{-1}$ and $\nu_{as}(\text{C=O})=1592 \text{ cm}^{-1}$) did not change significantly upon increasing the AA concentration. However, the presence of coordinated acetate groups cannot be entirely ruled out due to the appearance of small vibration bands at 1428 and 1564 cm^{-1} . Indeed, it is well established that Zr nanoMOFs can exhibit defects such as missing ligands or missing clusters, leading to the formation of open metal sites that are prone to interact with AA.^{37,49-50} These spectroscopic ellipsometry experiments showed that the adsorption of small amount of AA by a hydrophobic MOF does not strongly impact its water adsorption properties and thus preserves its adsorption selectivity towards AA. This confirms that UiO-66(Zr)-2CF₃ is a highly selective MOF for the capture of AA under humid conditions.

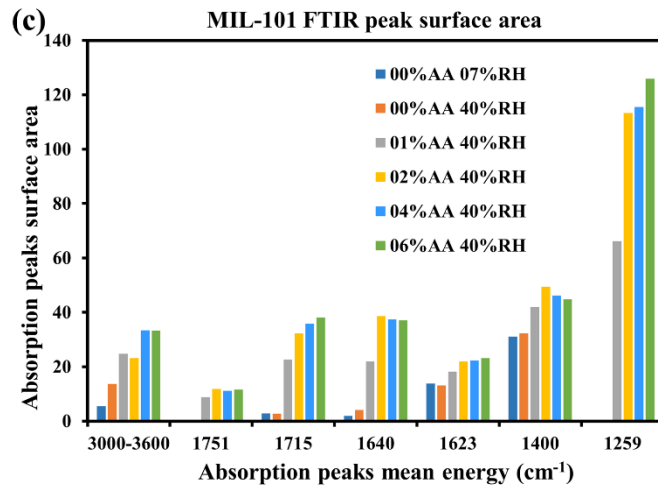
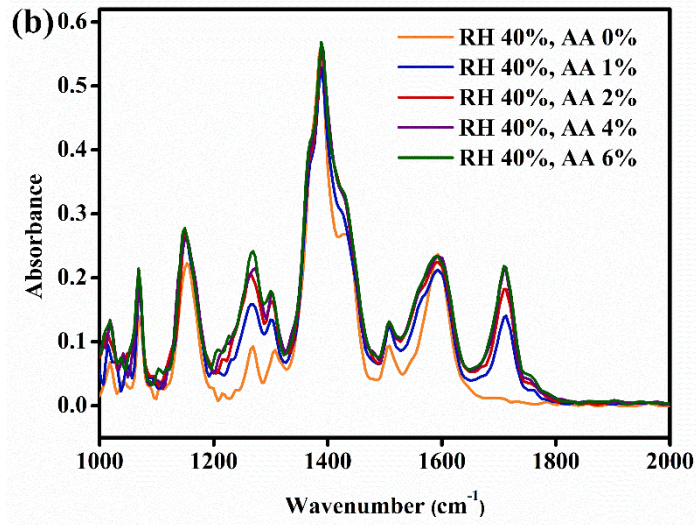
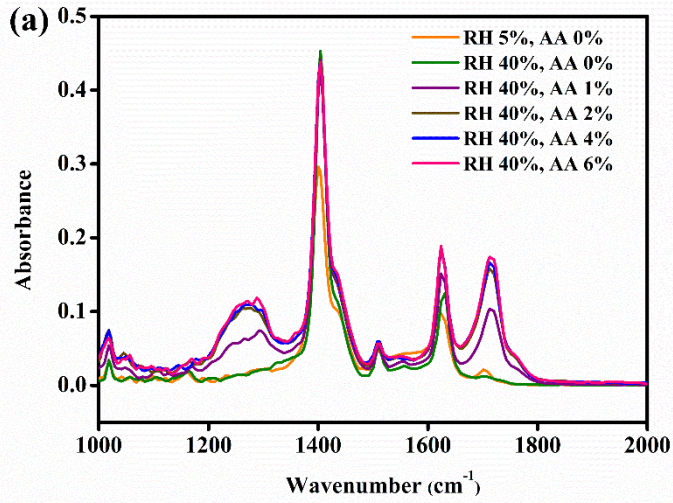


Figure 4 FT-IR spectra of thin films of a) MIL-101(Cr), b) UiO-66(Zr)-2CF₃ exposed to water/AA vapors of different composition acquired by using IR ellipsometer and c) FT-IR absorption bands surface area obtained from IRVASE spectra. Extinction coefficient are determined with a precision of 0.001

3.4. Adsorption/desorption cycling stability of thin films of MIL-101(Cr) and UiO-66(Zr)-2CF₃. To test the reversibility of the AA adsorption process in both MIL-101(Cr) and UiO-66(Zr)-2CF₃ films and thus their cycling stability, dynamic UVSE experiments were performed upon exposure of the films to continuous adsorption of AA and water vapors and desorption cycles (Figure 5). The cycles of AA/water were made of three steps: desorption of the films by heating at 120°C under air for 2 min, exposure of the films to water vapor (40% RH) and finally to a mixture of AA and water vapors (40% RH + 2, 4 or 6% P/P_{vapsat} of AA) (Figure 5c,d)). For comparison, nanoMOF films were also exposed to adsorption/desorption cycles in which films were alternatively desorbed at 120°C under air and exposed to pure AA vapor (2, 4 and 6% P/P_{vapsat} of AA in dry air) (Figure 5a,b)). It appears that the two selected MOF films behave differently. Once exposed to pure AA vapors at 2% P/P_{vapsat}, MIL-101(Cr) films exhibited the highest increase of refractive index evaluated at ~ 0.07 RIU/%_{AA} while UiO-66(Zr)-2CF₃ film shows a response of ~ 0.02 RIU/%_{AA} (Figure 5 a,b). Note that both MOF films present a fast AA adsorption kinetics since this change in RI is achieved upon adsorption of AA within less than 2 min. (Figure 5a,b)). The high optical response of MIL-101(Cr) is thus imparted by its higher pore volume. By varying the AA P/P_{vapsat} from 2 to 6%, a slight increase of refractive index was observed for MIL-101(Cr) films while the RI was almost constant for UiO-66(Zr)-2CF₃ films (Figures 5 a and b)). This arises from the significant difference of adsorption capacity between the mesoporous MIL-101(Cr) and microporous UiO-66(Zr)-2CF₃ materials. It can be assumed that UiO-66(Zr)-2CF₃ is saturated in this range of AA concentrations and consequently gives the same increase of RI. However, the optical response of MIL-101(Cr) upon water/AA exposure was shown not to be stable upon adsorption/desorption cycling (Figure 5c). If the first adsorption of water did not induce a significant increase of the RI, after a first cycle of water/AA mixture adsorption/desorption, a second exposure to water flow led to a more significant increase of RI than during the first exposure to water. Moreover, the increase of the RI due to the adsorption of AA was significantly lower than that after the first water/AA exposure cycle.

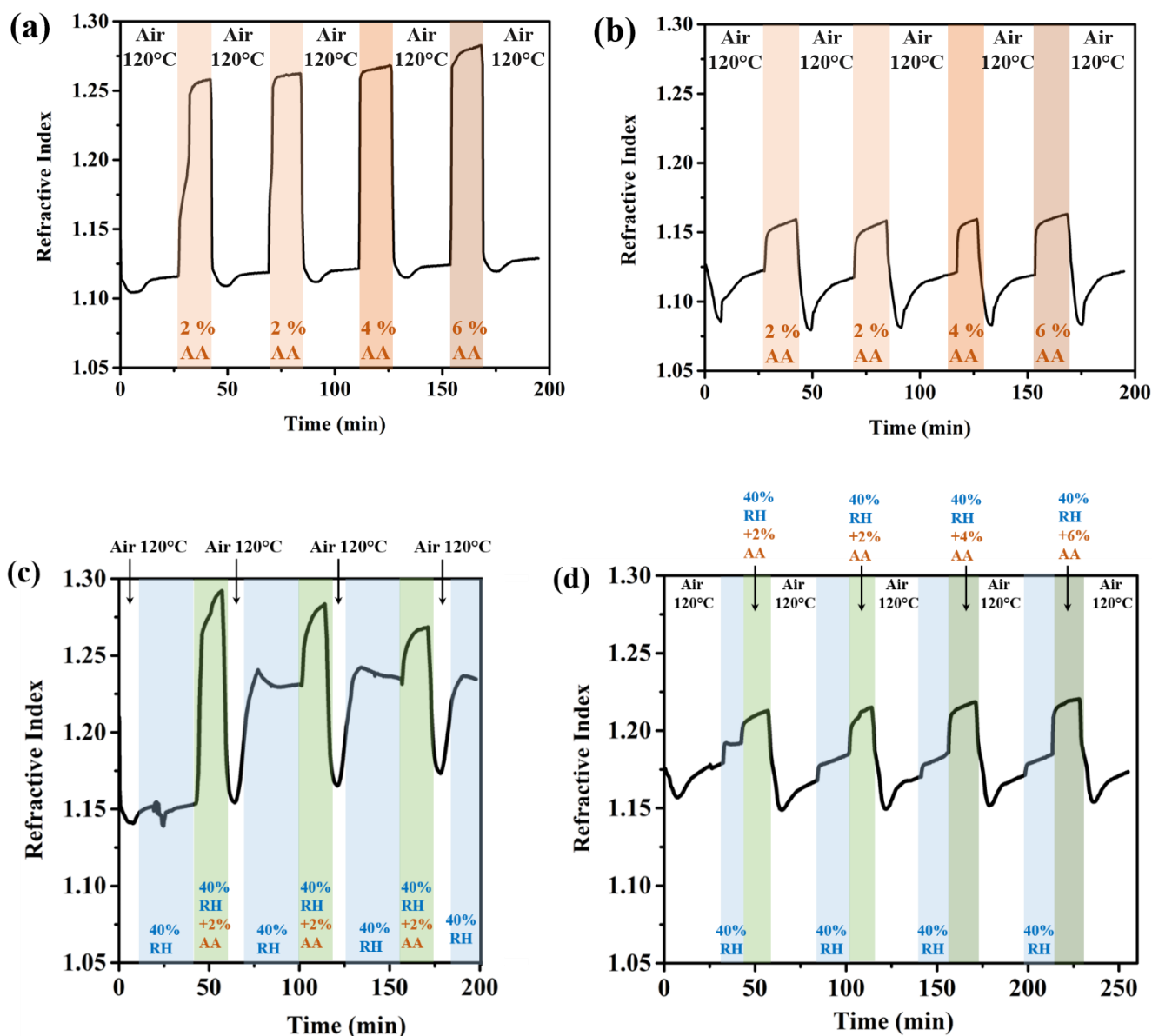


Figure 5. Cycling UVSE experiments on films of (a, c) MIL-101(Cr) and (b, d) UiO-66(Zr)-2CF₃ exposed to (a, b) AA vapors (2, 4 or 6 % P/P_{vapsat}) or desorption steps (120°C, 2 min, 18°C/min) or (c, d) water vapor at 40%RH, water (RH 40% RH) and AA (2, 4 or 6 % P/P_{vapsat}) vapors and desorption steps (120°C, 2 min, 18°C/min).

It can be assumed that over each cycle, water, AA or both molecules are trapped within the structure due to their cooperative co-adsorption process. Moreover, as shown by IRVASE, a significant amount of AA gets also coordinated to the Cr CUS of MIL-101(Cr). It was shown previously that a full desorption of coordinated water molecules from such type of Lewis acid site based MOF requires a prolonged exposure to high temperature and vacuum. One can assume that here the coordinated AA molecules are far from being fully desorbed after the rapid 120°C activation (e.g. a few minutes) which leads to this irreversible behavior. This material provides high RI increase but suffers from the impact of AA on its

hydrophilicity/hydrophobicity balance which also makes difficult its reuse after a first adsorption cycle. In contrast, the AA and AA/water adsorption/desorption processes of UiO-66(Zr)-2CF₃ are fully reversible showing the excellent cycling stability of this MOF upon AA adsorption in the presence of humidity as shown in Figure 5d. Moreover, the RI of a UiO-66(Zr)-2CF₃ film exposed to pure water is four times lower than that of a film exposed to a water/AA mixture while the concentration of AA is about 20 times lower than water. The films of UiO-66(Zr)-2CF₃ present thus the advantage to exhibit reversible and selective AA adsorption in the presence of humidity and consequently can be regenerated after heating at 120°C for a few minutes. As shown previously by molecular simulation, the high AA adsorption selectivity of this MOF arises from its chemical and microstructural features.¹⁹ Indeed, the presence of lipophilic -CF₃ groups grafted on the MOF backbone not only confers a high hydrophobic character but also enhances the interactions with AA. This MOF exhibits also an adequate pore size able to optimize the confinement of AA in the material.

4. CONCLUSIONS

The AA adsorption properties of three slightly hydrophobic MOFs (ZIF-8(Zn), MIL-101(Cr), and UiO-66(Zr)-2CF₃) were thoroughly characterized under humid ambient conditions by in situ UV-vis and FT-IR spectroscopic ellipsometry in the context of the preservation of cultural artefacts in museums. Stable colloidal suspensions of nanoMOFs were prepared for the processing of thin films of high optical quality. A strong degradation of ZIF-8(Zn) films was first evidenced upon exposure to humid AA vapor, possibly associated with the complexation of metal centers by AA molecules and the concomitant hydrolysis of metal-ligand bonds. However, the high value of $\Delta RI/\Delta C$ (with C being the AA concentration) measured revealed that the ZIF-8(Zn) film could be used as a single-use and highly sensitive AA sensor. Both thin films of MIL-101(Cr), and UiO-66(Zr)-2CF₃ were shown to be chemically stable once exposed to water/ AA vapors mixture. The AA adsorption capacity of MIL-101(Cr) was significantly higher than that of UiO-66(Zr)-2CF₃ as a result of its higher pore volume. However, MIL-101(Cr) presented a lower AA/H₂O adsorption selectivity as a result of a decrease of its hydrophobic character in the presence of AA vapor. A partial coordination of AA molecules on the CUS of MIL-101(Cr) was clearly shown by IRVASE and this further limited the regeneration of this material. In contrast, the water isotherm of UiO-66(Zr)-2CF₃ was slightly impacted by the presence of AA vapor due to its high hydrophobic character. This MOF presented a high AA adsorption selectivity and an excellent adsorption/desorption cycling stability upon exposure to continuous water/AA cycles. These two MOFs present complementary AA adsorption properties (high adsorption capacity for MIL-101(Cr) and high adsorption selectivity for UiO-66(Zr)-2CF₃) that could be exploited for the abatement of AA in CH environments depending on the rela-

tive concentration of AA and water. Note that the regeneration of the adsorbents in CH institutions (museums, archives, libraries) are generally not performed at the present time since it requires energy-consuming activation steps and thus some equipments that are not accessible in those institutions. This means that the low adsorption selectivity of MIL-101(Cr) is not a critical issue as soon as this MOF is commonly employed in CH institutions as a single-use CH adsorbent. In the future, the adsorption performance of these MOFs should be explored towards the competitive removal of a mixture of gaseous CCs (or VOCs) that is more representative of the real indoor environments of CH institutions.

ASSOCIATED CONTENT

The Supporting Information is available free of charge at <https://pubs.acs.org/doi/.....>

Further details on the synthesis of MOFs, processing of MOF thin films and structural characterization (PXRD, FTIR, TGA, N₂ porosimetry, TEM, HAADF-STEM, ...), UV-vis and FT-IR spectroscopic ellipsometry.

AUTHOR INFORMATION

Corresponding Author

Christian Serre - Institut des Matériaux Poreux de Paris (IMAP), Ecole Normale Supérieure de Paris, ESPCI Paris, CNRS, PSL University, 75005 Paris, France. Email : christian.serre@ens.fr Orcid.org/ 0000-0003-3040-2564

Cédric Boissière - Sorbonne Université, CNRS, Collège de France, UMR Chimie de la Matière Condensée de Paris, Paris, France. Email : cedric.boissiere@upmc.fr Orcid.org/ 0000-0003-1212-6850

Nathalie Steunou - Institut Lavoisier de Versailles, UMR CNRS 8180, Université de Versailles St Quentin en Yvelines, Université Paris Saclay, Versailles, France. Email : nathalie.steunou@uvsq.fr. Email : nathalie.steunou@uvsq.fr Orcid.org/ 0000-0002-7049-7388.

Authors

Sanchari Dasgupta - Institut Lavoisier de Versailles, UMR CNRS 8180, Université de Versailles St Quentin en Yvelines, Université Paris Saclay, Versailles, France. Orcid.org/ 0000-0003-4997-5258

Subharanjan Biswas - Institut Lavoisier de Versailles, UMR CNRS 8180, Université de Versailles St Quentin en Yvelines, Université Paris Saclay, Versailles, France. Orcid.org/ 0000-0002-1608-4240

Kevin Dedecker - Institut Lavoisier de Versailles, UMR CNRS 8180, Université de Versailles St Quentin en Yvelines, Université Paris Saclay, Versailles, France. & Centre de Recherche sur la Conservation, USR 3224: CNRS-MNHN-MCC, Sorbonne Universités, 36 rue Geoffroy-Saint-Hilaire, 75005 Paris Cedex, France. Orcid.org/ 0000-0002-8039-9925

Eddy Dumas - Institut Lavoisier de Versailles, UMR CNRS 8180, Université de Versailles St Quentin en Yvelines, Université Paris Saclay, Versailles, France. Orcid.org/ 0000-0001-7156-6907

Nicolas Menguy - Sorbonne Université, UMR CNRS 7590, MNHN, IRD, Institut de Minéralogie, de Physique des Matériaux et de Cosmochimie, IMPMC, Paris, France. Orcid.org/ 0000-0003-4613-2490

Bruno Berini, Groupe d'Etudes de la Matière Condensée, UMR CNRS 8635, Université de Versailles St Quentin en Yvelines, Université Paris Saclay 78035 Versailles, France.

Bertrand Lavedrine, Centre de Recherche sur la Conservation, UAR CNRS 3224, Muséum National d'Histoire Naturelle, 75005 Paris, France.

Author Contributions

|| These authors contributed equally.

ACKNOWLEDGMENT

This work was supported by the Ecole Universitaire de recherche PSGS HCH Humanities, Creation, Heritage, Investissement d'Avenir ANR-17-EURE-0021 - Fondation des sciences du patrimoine. This work has been sponsored by the Ile-de-France Region in the framework of Respire, the Île-de-France network of Excellence in Porous Solids. The authors acknowledge Ali Saad for SEM experiments.

REFERENCES

- (1) Dupont, A. L.; Tetreault, J. Cellulose Degradation in an Acetic Acid Environment. *Stud. Conserv.* **2000**, *45*, 201-210.
- (2) T etreault, J. Airborne Pollutants in Museums, Galleries and Archives: Risk Assessment, Control Strategies and Preservation Management. Canadian Conservation Institute: Ottawa, 2003; Chapter 3, p 31.
- (3) Gibson, L. T.; Ewlad-Ahmed, A.; Knight, B.; Horie, V.; Mitchell, G.; Robertson, C. J. Measurement of Volatile Organic Compounds Emitted in Libraries and Archives: An Inferential Indicator of Paper Decay? *Chem. Cent. J.* **2012**, *6*, 42.
- (4) Lopez-Aparicio, S.; Gr ontoft, T.; Dahlin, E. Air Quality Assessment in Cultural Heritage Institutions using EWO Dosimeters. *E-Preserv. Sci.* **2010**, *7*, 96-101.
- (5) Hackney, S. Colour Measurement of Acid-Detector Strips for the Quantification of Volatile Organic Acids in Storage Conditions. *Stud. Conserv.* **2016**, *61*, 55-69.
- (6) Grzywacz, C. M. 10th Triennial Meeting, Washington DC, 22-27/8/1993; ICOM Committee for Conservation: Washington DC, 1993; p 610.
- (7) Gibson, L. T.; Watt, C. M. Acetic and Formic Acids Emitted from Wood Samples and Their Effect on Selected Materials in Museum Environments. *Corros. Sci.* **2010**, *52*, 172-178.
- (8) L opez-Aparicio, S.; Gr ontoft, T.; Odlyha, M.; Dahlin, E.; Mottner, P.; Thickett, D.; Ryhl-Svendsen, M.; Schmidbauer, N.; Scharff, M. Measurement of Organic and Inorganic Pollutants in Microclimate Frames for Paintings. *E-Preserv. Sci.* **2010**, *7*, 59-70.
- (9) Cruz, A. J.; Pires, J.; Carvalho, A.; Brotas de Carvalho, M. Adsorption of Acetic Acid by Activated Carbons, Zeolites, and Other Adsorbent Materials Related with the Preventive Conservation of Lead Objects in Museum Showcases. *J. Chem. Eng. Data* **2004**, *49*, 725-731.
- (10) Al Mohtar, A.; Pinto, M. L.; Neves, A.; Nunes, S.; Zappi, D.; Varani, G.; Ramos, A. M.; Melo, M. J.; Wallaszkovits, N.; Lahoz Rodrigo, J. I.; Herlt, K.; Lopes, J. Decision making based on hybrid modeling approach applied to cellulose acetate based historical films conservation. *Scientific reports* **2021**, *11*, 16074.
- (11) Na, C.-J.; Yoo, M.-J.; Tsang, D. C. W.; Kim, H. W.; Kim, K.-H. High-Performance Materials for Effective Sorptive Removal of Formaldehyde in Air. *J. Hazard. Mater.* **2019**, *366*, 452-465.
- (12) Suresh, S.; Badosz, T. J. Removal of Formaldehyde on Carbon -Based Materials: A Review of the Recent Approaches and Findings. *Carbon* **2018**, *137*, 207-221.
- (13) Yuan, H.; Tao, J.; Li, N.; Karmakar, A.; Tang, C.; Cai, H.; Pennycook, S. J.; Singh, N.; Zhao, D. On-Chip Tailorability of Capacitive Gas Sensors Integrated with Metal–Organic Framework Films. *Angew. Chem. Int. Ed.* **2019**, *58*, 14089-14094.
- (14) Bhattarai, D. P.; Pant, B.; Acharya, J.; Park, M.; Ojha, G. P. Recent Progress in Metal-Organic Framework-Derived Nanostructures in the Removal of Volatile Organic Compounds. *Molecules* **2021**, *26*.
- (15) Binaeian, E.; El-Sayed, E. S. M.; Matikolaie, M. K.; Yuan, D. Q. Experimental Strategies on Enhancing Toxic Gases Uptake of Metal-Organic Frameworks. *Coord. Chem. Rev.* **2021**, *430*, 213738.
- (16) Li, X. Q.; Zhang, L.; Yang, Z. Q.; Wang, P.; Yan, Y. F.; Ran, J. Y. Adsorption materials for volatile organic compounds (VOCs) and the key factors for VOCs adsorption process: A review. *Sep. Purif. Technol.* **2020**, *235*, 116213.
- (17) Bo, R.; Taheri, M.; Liu, B.; Ricco, R.; Chen, H.; Amenitsch, H.; Fusco, Z.; Tsuzuki, T.; Yu, G.; Ameloot, R.; Falcaro, P.; Tricoli, A. Hierarchical Metal-Organic Framework Films with Controllable Meso/Macroporosity. *Adv. Sci.* **2020**, *7*, 2002368.

- (18) Li, J.; Bhatt, P. M.; Li, J.; Eddaoudi, M.; Liu, Y. Recent Progress on Microfine Design of Metal–Organic Frameworks: Structure Regulation and Gas Sorption and Separation. *Adv. Mater.* **2020**, *32*, 2002563.
- (19) Dedecker, K.; Pillai, R. S.; Nouar, F.; Pires, J.; Steunou, N.; Dumas, E.; Maurin, G.; Serre, C.; Pinto, M. L. Metal–Organic Frameworks for Cultural Heritage Preservation: The Case of Acetic Acid Removal. *ACS Appl. Mater. Interfaces* **2018**, *10*, 13886–13894.
- (20) Bobbitt, N. S.; Mendonca, M. L.; Howarth, A. J.; Islamoglu, T.; Hupp, J. T.; Farha, O. K.; Snurr, R. Q. Metal–Organic Frameworks for the Removal of Toxic Industrial Chemicals and Chemical Warfare Agents. *Chem. Soc. Rev.* **2017**, *46*, 3357–3385.
- (21) Castells-Gil, J.; Padial, N. M.; Almora-Barrios, N.; Gil-San-Millan, R.; Romero-Angel, M.; Torres, V.; da Silva, I.; Vieira, B. C. J.; Waerenborgh, J. C.; Jagiello, J.; Navarro, J. A. R.; Tatay, S.; Marti-Gastaldo, C. Heterometallic Titanium–Organic Frameworks as Dual-Metal Catalysts for Synergistic Non-buffered Hydrolysis of Nerve Agent Simulants. *Chem* **2020**, *6*, 3118–3131.
- (22) He, T.; Kong, X. -J.; Bian, Z. -X.; Zhang, Y. -Z.; Si, G. -R.; Xie, L. -H.; Wu, X. -Q.; Huang, H.; Chang, Z.; Bu, X. -H.; Zaworotko, M. J.; Nie, Z. -R.; Li, J. -R. Trace Removal of Benzene Vapour Using Double-Walled Metal–Dipyrazolate Frameworks. *Nat. Mater.* **2022**, *21*, 689–695.
- (23) Vikrant, K.; Qu, Y.; Szulejko, J. E.; Kumar, V.; Vellingiri, K.; Boukhvalov, D. W.; Kim, T.; Kim, K. H. Utilization of Metal–Organic Frameworks for the Adsorptive Removal of an Aliphatic Aldehyde Mixture in the Gas Phase. *Nanoscale* **2020**, *12*, 8330–8343.
- (24) Vellingiri, K.; Deng, Y. X.; Kim, K. H.; Jiang, J. J.; Kim, T.; Shang, J.; Ahn, W. S.; Kukkar, D.; Boukhvalov, D. W. Amine-Functionalized Metal–Organic Frameworks and Covalent Organic Polymers as Potential Sorbents for Removal of Formaldehyde in Aqueous Phase: Experimental Versus Theoretical Study. *ACS Appl. Mater. Interfaces* **2019**, *11*, 1426–1439.
- (25) Vikrant, K.; Kim, K. H.; Kumar, V.; Giannakoudakis, D. A.; Boukhvalov, D. W. Adsorptive Removal of an Eight -Component Volatile Organic Compound Mixture by Cu-, Co-, and Zr-Metal–Organic Frameworks: Experimental and Theoretical Studies. *Chem. Eng. J.* **2020**, *397*, 125391.
- (26) Zhao, Q. Y.; Du, Q. X.; Yang, Y.; Zhao, Z. Y.; Cheng, J.; Bi, F. K.; Shi, X. Y.; Xu, J. C.; Zhang, X. D. Effects of Regulator Ratio and Guest Molecule Diffusion on VOCs Adsorption by Defective UiO-67: Experimental and Theoretical Insights. *Chem. Eng. J.* **2022**, *433*, 134510.
- (27) Wang, B.; Lv, X. -L.; Feng, D.; Xie, L. -H.; Zhang, J.; Li, M.; Xie, Y.; Li, J. -R.; Zhou, H. -C. Highly Stable Zr(IV)-Based Metal–Organic Frameworks for the Detection and Removal of Antibiotics and Organic Explosives in Water. *J. Am. Chem. Soc.* **2016**, *138*, 6204–6216.
- (28) Xie, L. -H.; Liu, X. -M.; He, T.; Li, J. -R. Metal–Organic Frameworks for the Capture of Trace Aromatic Volatile Organic Compounds. *Chem* **2018**, *4*, 1911–1927.
- (29) Tietze, M. L.; Obst, M.; Arnauts, G.; Wauteraerts, N.; Rodriguez-Hermida, S.; Ameloot, R. Parts-per-Million Detection of Volatile Organic Compounds via Surface Plasmon Polaritons and Nanometer-Thick Metal–Organic Framework Films. *ACS Appl. Nano Mater.* **2022**, *5*, 5006–5016.
- (30) Demessence, A.; Horcajada, P.; Serre, C.; Boissiere, C.; Grosso, D.; Sanchez, C.; Férey, G. Elaboration and Properties of Hierarchically Structured Optical Thin Films of MIL-101(Cr). *Chem. Commun.* **2009**, 7149–7151.
- (31) Demessence, A.; Boissière, C.; Grosso, D.; Horcajada, P.; Serre, C.; Férey, G.; Soler-Illia, G. J. A. A.; Sanchez, C. Adsorption Properties in High Optical Quality NanoZIF-8 Thin Films with Tunable Thickness. *J. Mater. Chem.* **2010**, *20*, 7676–7681.
- (32) Ikigaki, K.; Okada, K.; Tokudome, Y.; Toyao, T.; Falcaro, P.; Doonan, C. J.; Takahashi, M. MOF-on-MOF: Oriented Growth of Multiple Layered Thin Films of Metal–Organic Frameworks. *Angew. Chem. Int. Ed. Engl.* **2019**, *58*, 6886–6890.
- (33) Castilla-Casadiago, D. A.; Pinzon-Herrera, L.; Perez-Perez, M.; Quiñones-Colón, B. A.; Suleiman, D.; Almodovar, J. Simultaneous Characterization of Physical, Chemical, and Thermal Properties of

- Polymeric Multilayers using Infrared Spectroscopic Ellipsometry. *Colloids Surf. A: Physicochem. Eng. Asp.* **2018**, *553*, 155-168.
- (34) Ferey, G.; Mellot-Draznieks, C.; Serre, C.; Millange, F.; Dutour, J.; Surble, S.; Margiolaki, I. A Chromium Terephthalate-Based Solid with Unusually Large Pore Volumes and Surface Area. *Science* **2005**, *309*, 2040-2042.
- (35) Banerjee, R.; Phan, A.; Wang, B.; Knobler, C.; Furukawa, H.; O'Keeffe, M.; Yaghi, O. M. High-Throughput Synthesis of Zeolitic Imidazolate Frameworks and Application to CO₂ Capture. *Science* **2008**, *319*, 939-943.
- (36) Zhu, X.; Gu, J.; Wang, Y.; Li, B.; Li, Y.; Zhao, W.; Shi, J. Inherent Anchorages in UiO-66 Nanoparticles for Efficient Capture of Alendronate and Its Mediated Release. *Chem. Commun.* **2014**, *50*, 8779-8782.
- (37) Shearer, G. C.; Chavan, S.; Bordiga, S.; Svelle, S.; Olsbye, U.; Lillerud, K. P. Defect Engineering: Tuning the Porosity and Composition of the Metal–Organic Framework UiO-66 via Modulated Synthesis. *Chem. Mater.* **2016**, *28*, 3749-3761.
- (38) Forgan, R. S. Modulated Self-assembly of Metal-Organic Frameworks. *Chem. Sci.* **2020**, *11*, 4546-4562.
- (39) DeStefano, M. R.; Islamoglu, T.; Garibay, S. J.; Hupp, J. T.; Farha, O. K. Room-Temperature Synthesis of UiO-66 and Thermal Modulation of Densities of Defect Sites. *Chem. Mater.* **2017**, *29*, 1357-1361.
- (40) Shearer, G. C.; Vitillo, J. G.; Bordiga, S.; Svelle, S.; Olsbye, U.; Lillerud, K. P. Functionalizing the Defects: Postsynthetic Ligand Exchange in the Metal Organic Framework UiO-66. *Chem. Mater.* **2016**, *28*, 7190-7193.
- (41) Benzaqui, M.; Semino, R.; Carn, F.; Tavares, S. R.; Menguy, N.; Giménez-Marqués, M.; Bellido, E.; Horcajada, P.; Berthelot, T.; Kuzminova, A. I.; Dmitrenko, M. E.; Penkova, A. V.; Roizard, D.; Serre, C.; Maurin, G.; Steunou, N. Covalent and Selective Grafting of Polyethylene Glycol Brushes at the Surface of ZIF-8 for the Processing of Membranes for Pervaporation. *ACS Sustain. Chem. Eng.* **2019**, *7*, 6629-6639.
- (42) Zhang, H.; James, J.; Zhao, M.; Yao, Y.; Zhang, Y.; Zhang, B.; Lin, Y. S. Improving Hydrostability of ZIF-8 Membranes via Surface Ligand Exchange. *J. Membr. Sci.* **2017**, *532*, 1-8.
- (43) Zhang, H.; Liu, D.; Yao, Y.; Zhang, B.; Lin, Y. S. Stability of ZIF-8 Membranes and Crystalline Powders in Water at Room Temperature. *J. Membr. Sci.* **2015**, *485*, 103-111.
- (44) Khutia, A.; Rammelberg, H. U.; Schmidt, T.; Henninger, S.; Janiak, C. Water Sorption Cycle Measurements on Functionalized MIL-101Cr for Heat Transformation Application. *Chem. Mater.* **2013**, *25*, 790-798.
- (45) Boudot, M.; Ceratti, D. R.; Faustini, M.; Boissière, C.; Grosso, D. Alcohol-Assisted Water Condensation and Stabilization into Hydrophobic Mesoporosity. *J. Phys. Chem. C.* **2014**, *118*, 23907-23917.
- (46) Fu, J. H.; Zhong, Z.; Xie, D.; Guo, Y. J.; Kong, D. X.; Zhao, Z. X.; Zhao, Z. X.; Li, M. SERS-Active MIL-100(Fe) Sensory Array for Ultrasensitive and Multiplex Detection of VOCs. *Angew. Chem. Int. Ed.* **2020**, *59*, 20489-20498.
- (47) Gkaniatsou, E.; Ricoux, R.; Kariyawasam, K.; Stenger, I.; Fan, B.; Ayoub, N.; Salas, S.; Patriarche, G.; Serre, C.; Mahy, J.-P.; Steunou, N.; Sicard, C. Encapsulation of Microperoxidase-8 in MIL-101(Cr)-X Nanoparticles: Influence of Metal–Organic Framework Functionalization on Enzymatic Immobilization and Catalytic Activity. *ACS Appl. Nano Mater.* **2020**, *3*, 3233-3243.
- (48) Biswas, S.; Haouas, M.; Freitas, C.; Soares, C. V.; Al Mohtar, A.; Saad, A.; Zhao, H.; Mouchaham, G.; Livage, C.; Carn, F.; Menguy, N.; Maurin, G.; Pinto, M. L.; Steunou, N. Engineering of Metal-Organic Frameworks/Gelatin Hydrogel Composites Mediated by the Coacervation Process for the Capture of Acetic Acid. *Chem. Mater.* **2022**, *34*, 9760-9774.

- (49) Chen, Z.; Feng, L.; Liu, L.; Bhatt, P. M.; Adil, K.; Emwas, A. H.; Assen, A. H.; Belmabkhout, Y.; Han, Y.; Eddaoudi, M. Enhanced Separation of Butane Isomers via Defect Control in a Fumarate/Zirconium-Based Metal Organic Framework. *Langmuir* **2018**, *34*, 14546-14551.
- (50) Dai, S.; Nouar, F.; Zhang, S.; Tissot, A.; Serre, C. One-Step Room-Temperature Synthesis of Metal(IV) Carboxylate Metal-Organic Frameworks. *Angew. Chem. Int. Ed.* **2021**, *60*, 4282-4288.

Table of Contents artwork here

